BIOMOLECULES & THERAPEUTICS

Original Article
Biomol Ther 24(1), 85-93 (2016)

Anti-Melanogenic Potentials of Nanoparticles from Calli of Resveratrol-Enriched Rice against UVB-Induced Hyperpigmentation in Guinea Pig Skin

Taek Hwan Lee[1], Ji Hee Kang[2], Jae Ok Seo[2], So-Hyeon Baek[3], Sang Hyun Moh[4], Jae Kyoung Chae[2], Yong Un Park[2], Young Tag Ko[2] and Sun Yeou Kim[2,5,6,*]

[1]College of Pharmacy, Yonsei University, Incheon 21983,
[2]College of Pharmacy, Gachon University, Incheon 21936,
[3]National Institute of Crop Science, Rural Development Administration, Iksan 54663,
[4]Anti-aging Research Institute, BIO-FD&C Co., LTD, Incheon 21990,
[5]Gachon Medical Research Institute, Gil Medical Center, Inchon 21565,
[6]Gachon Institute of Pharmaceutical Science, Gachon University, Incheon 21936, Republic of Korea

Abstract

We already reported that genetically engineered resveratrol-enriched rice (RR) showed to down-regulate skin melanogenesis. To be developed to increase the bioactivity of RR using calli from plants, RR was adopted for mass production using plant tissue culture technologies. In addition, high-pressure homogenization (HPH) was used to increase the biocompatibility and penetration of the calli from RR into the skin. We aimed to develop anti-melanogenic agents incorporating calli of RR (cRR) and nanoparticles by high-pressure homogenization, examining the synergistic effects on the inhibition of UVB-induced hyperpigmentation. Depigmentation was observed following topical application of micro-cRR, nano-calli of normal rice (cNR), and nano-cRR to ultraviolet B (UVB)-stimulated hyperpigmented guinea pig dorsal skin. Colorimetric analysis, tyrosinase immunostaining, and Fontana-Masson staining for UVB-promoted melanin were performed. Nano-cRR inhibited changes in the melanin color index caused by UVB-promoted hyperpigmentation, and demonstrated stronger anti-melanogenic potential than micro-cRR. In epidermal skin, nano-cRR repressed UVB-promoted melanin granules, thereby suppressing hyperpigmentation. The UVB-enhanced, highly expressed tyrosinase in the basal layer of the epidermis was inhibited by nano-cRR more prominently than by micro-cRR and nano-cNR. The anti-melanogenic potency of nano-cRR also depended on pH and particle size. Nano-cRR shows promising potential to regulate skin pigmentation following UVB exposure.

Key Words: Plant tissue culture, High-pressure homogenization, Melanogenesis, Resveratrol-enriched rice, Nanoparticles

INTRODUCTION

Resveratrol-enriched rice (RR) was first developed by the Rural Development Administration of Korea using genetic engineering techniques. Our group has demonstrated that RR regulated metabolic syndrome and related diseases, as opposed to resveratrol or rice, through synergistic interactions (Baek *et al*., 2013; Baek *et al*., 2014). In addition, we have also reported that RR positively down-regulated skin melanogenesis in ultraviolet B (UVB)-induced models (Lee *et al*., 2014b). Therefore, RR may be a promising material for the regulation of skin pigmentation via UVB exposure. Developers of cosmeceuticals and nutraceuticals are becoming increasingly interested in using unusual natural products such as RR. However, one of the most challenging issues facing natural products is the standardization of materials in terms of uniformity and safety. It is difficult to control many variable factors for the mass production of an active compound from natural products. As part of an effort to overcome the limitations, there is a rising interest in studying biotechnical-based approaches such as plant tissue culture, which makes mass production possible. This process leads not only to an effectively low cost,

Open Access **http://dx.doi.org/10.4062/biomolther.2015.165**

Received Oct 13, 2015 **Revised** Oct 26, 2015 **Accepted** Nov 17, 2015
Published online Jan 1, 2016

***Corresponding Author**
E-mail: sunnykim@gachon.ac.kr
Tel: +82-32-899-6411, Fax: +82-32-899-8962

but is also not affected by geographical and seasonal factors during plant growth (Jafarain *et al*., 2014). Researchers have constantly tried to grow reproducible plants with properties similar to or better than those of wild plants containing active compounds, through the plant tissue culture system (Siddique *et al*., 2014). To date, several studies on the biological activities of plant calli have been reported. Callus produced by *Moringa oleifera* Lam. showed cytotoxic effects in HeLa cells (Jafarain *et al*., 2014), while callus produced by *Heliotropiumindicum* Linn. showed anti-oxidant activities (Kumar *et al*., 2014) and callus produced by *Oryza sativa* showed anti-cancer effects (Deshpande *et al*., 2012). These bioactive products produced by *in vitro* culture systems are recognized as commercial natural sources (Pandey *et al*., 2015). However, even though they have a high potential for application, plant calli are currently not widely utilized in commercial products. The most conventional method linked with extraction using natural products is solvent extraction. In a previous study, RR was extracted with methanol and the presence of resveratrol constituents was tested (Lee *et al*., 2014b). However, with the use of methanol, the extraction yield of RR was very low at 0.1%. When the case of extraction using water, even though the extraction efficiency of RR was increased at 10%, resveratrol could not be detected under such conditions (Quan *et al*., 2012). Therefore, a new approach needs to be developed to increase the bioactivity of RR using calli from plants. RR was adopted for mass production using plant tissue culture technologies. In addition, high-pressure homogenization (HPH) was used to increase the biocompatibility and penetration of the calli from RR into the skin. We hypothesized that the calli produced from RR would be more effective against skin hyperpigmentation than the RR extract itself. Recently, biotechnology associated with nanomaterials has progressed rapidly and has been applied to various products, including cosmetics. Particularly, regulations regarding the safety, bioactivity, and penetration of nanomaterials in cosmetics have been a great focus. To produce nanosuspensions (Merisko-Liversidge and Liversidge 2011), one of the most representative methods is high-pressure homogenization (HPH). Current industrial, pilot, or lab scale high-pressure homogenizers, equipped with plunger-type pumps and valves or nozzles made from abrasion-resistant ceramics or hard gemstones, may be used. The technology for nozzle-equipped high-pressure homogenizers was initially developed for water jet cutting applications. In this case, homogenization is achieved using a high-pressure pump, connected to an attenuator to reduce pressure fluctuations. The homogenization effect in high-pressure homogenizers can be attributed to improvements in physical phenomena. In particular, the cell wall, organelles, and cell membrane are completely disrupted by HPH (Palmero *et al*., 2015). Nanosuspension technology based on HPH can decrease particle sizes down to the nanometer range and increase surface area, which can result in an enhanced dissolution rate and bioavailability (Shelar *et al*., 2013; Karadag *et al*., 2014).We expect that the secretion of resveratrol from calli will be increased by the HPH process, leading to improved biocompatibility and skin penetration. Here, we describe the potential activities of nanomaterials by processing calli from RR. We examine the actual usage of nanomaterials in cosmetics based on an analysis of the existing nanomaterials used for the skin, and we assess the skin depigmentation activity of nano-sized calli from RR in UVB-induced hyperpigmented guinea pigs.

MATERIALS AND METHODS

Sterilization of seeds and callus induction

Mature seeds were sterilized with 70% (v/v) ethanol for 1 min and 2% sodium hypochlorite (NaOCl) for 1 h. The surface of the seeds was washed 4-5 times with sterile distilled water. The seeds were then inoculated in 2N6 medium (3.95 g/L N6 salt, 30 g/L sucrose, 1 g/L casamino acid, 2 mg/L 2,4-D, 2 g/L phytagel, pH 5.6-5.7) in petri dishes and incubated at 25°C in the dark for 3 weeks for callus induction.

Preparation of micro-cRR and nano-cRR

Calli of RR (cRR) were ground finely by constant trituration using a mortar and pestle. The ground cRR (200 mg) was dispersed in 5 mL of water, resulting in micro-cRR. The micro-cRR was further size-reduced by a probe sonicator at 40 amp for 5 min (VCX 750, Sonics & Materials, USA). It was then subjected 20 times to HPH (EmulsiFlex-B15, Avestin, Canada), resulting in nano-cRR. The resulting suspensions of cRR were analyzed for particle size distribution and zeta potentials using dynamic light scattering (ELSZ-1000, Otsuka Electronics Co, Japan).

In vitro release studies

The cumulative release of resveratrol from micro-cRR and nano-cRR was measured using the dialysis bag diffusion technique. Briefly, micro-cRR or nano-cRR corresponding to 10 mg of cRR was dispersed in 1 mL of buffers with varying pH of 1.2, 4.5, and 7.4, and separately transferred to a mini dialysis kit (molecular weight cut-off: 12-14 kDa). The dialysis kit was sealed at both ends and immersed in 2 mL of receptor medium containing 0.2% Tween 80. Samples were shaken horizontally in a shaker at 37 ± 1°C and 50 strokes per minute. At predefined time intervals (0, 0.5, 1, 2, 3, 4, 6, 8, 12, and 24 h), 2 mL of the release medium was taken from the receptor compartment and replaced with the same volume of fresh medium to maintain sink conditions. After dividing the samples into fractions of 1 mL, all collected samples were freeze-dried. Lyophilized samples were resuspended in 250 μL of ethyl acetate containing curcumin as an internal standard and vortexed for 1 min. The suspensions were centrifuged at 10,000 ×g for 10 min at 4°C, and the organic phase of the supernatant was transferred to new tubes. The supernatant was removed by vacuum evaporation. The residues were reconstituted with 20 μL of mobile phase and transferred to vials for LC-MS/MS analysis.

Animals

Male brownish A1 guinea pigs aged five weeks and weighting 270-300 g (n=4), obtained from Japan Kiwa Laboratory Animals Co., Ltd. (Wakayama, Japan), were used. All animal experiments were approved by the Institutional Animal Care and Use Committee of Korea Conformity Laboratories (IA13-00229). Breeding took place at a temperature of 22 ± 1°C, a humidity of 60 ± 5%, and in a 12 h-12 h dark-light cycle. After one week of quarantine, the guinea pigs were acclimated to individual cages. During the experimental period, food and water were given ad libitum. The animal study was performed according to the internationally accepted ethical principles of laboratory animal use and care.

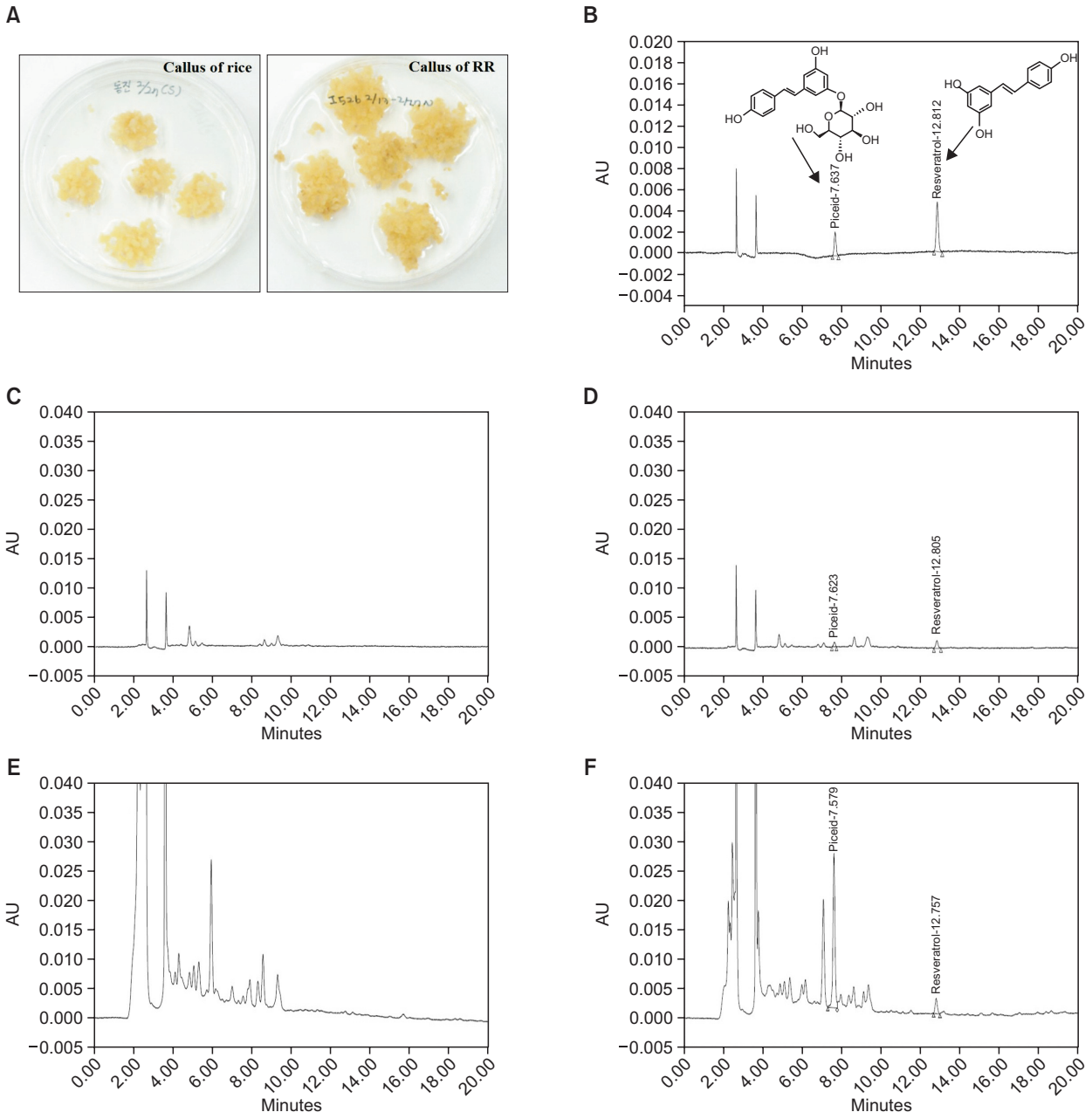

Fig. 1. The callus induction of RR. (A) Calli derived from rice (left) and RR (right). Representative HPLC chromatogram for quantification of piceid and resveratrol: (B) standard; (C) normal rice (NR); (D) resveratrol-enriched rice (RR); (E) callus of normal rice (cNR); (F) callus of resveratrol-enriched rice (cRR).

UVB-induced pigmentation of the guinea pig and sample treatment

Ultraviolet (UV) irradiation experiments were performed under a BLX-312 UV irradiation system (VilberLourmat, Marne-La-Valleée, France). Artificial UVB irradiation was created with five UVB-emitting lamps (UVB VilberLourmat T-8M with peak irradiance at 302 nm). The dorsal hair of each guinea pig was removed and exposed to 390 mJ/cm^2 UVB irradiation three times a week for two weeks. Various samples were dissolved in a mixture of propylene glycol, ethanol, and water (6:3:1, v/v). After UVB-induced pigmentation, the sample solution was topically applied to areas (2 cm × 2 cm) on the dorsal skin once a day for 15 days. The skin color index was observed using Dermalab® Combo system (Cortex Technology ApS, Hudsund, Denmark) during the treatment period.

Fontana-Masson stain

The Fontana-Masson silver stain for detecting melanin was performed according to previously described methods (Lee *et al*., 2014a). In brief, the biopsied dorsal skin was fixed in 4% paraformaldehyde for 24 h and embedded in paraffin. The embedded paraffin block was cut at a thickness of approximately

4 μm and stained with Fontana-Masson staining solution (IHC WORLD, GA, USA). The stained slides were examined under a light microscope.

Immunohistochemistry

The 4-μm thick sections were deparaffinized using xylene and rehydrated using a graded series of alcohol. Antigen retrieval was performed using 20 μg/mL proteinase (in PBS) for 20 min at 37°C. The sections were then incubated in 3% H_2O_2 in PBS for 15 min to block endogenous peroxidase activity. The slides were incubated overnight at 4°C with primary antibodies against tyrosinase, TRP-1, and TRP-2 (Santa Cruz Biotechnology Inc., CA, USA). Sections were then incubated with biotinylated secondary antibodies (Vector Laboratory, Piscataway, NJ, USA) for 20 min at room temperature. After washing in PBS, the slides were incubated in Vectastain ABC reagent (Vector Laboratory, Piscataway, NJ, USA) for 30 min. The color was developed with 3,3′-diaminobenzidine (Vector Laboratory, Piscataway, NJ, USA). Slides were counterstained with hematoxylin for 3 min.

Sample extraction and LC-MS/MS analysis for contents of resveratrol in skin tissue

Samples for liquid chromatography-mass spectrometry (LC-MS/MS) analysis were prepared by liquid-liquid extraction. The treated tissue samples were collected and homogenized by Bioprep-24 homogenizer (Bioand, Seoul, Korea) after addition of PBS which is equivalent to the weight of each tissue used. The homogenized tissues were then sonicated by a Bioruptor ultra-sonication (Cosmobio, Tokyo, Japan). 10 μL of samples were resuspended in 250 μL of ethyl acetate containing curcumin as an internal standard and vortexed for 1 min. The suspensions were centrifuged at 10,000×g for 10 min at 4°C, and the organic phase of the supernatant was transferred to new tubes. The supernatant was removed by vacuum evaporation. The residues were reconstituted with 20 μL of mobile phase and transferred to vials for LC-MS/MS analysis.

LC-MS/MS conditions

The LC-MS/MS system consisted of an Agilent LC 1100 series (Agilent Technologies, CA, USA) binary pump, a vacuum degasser, and an auto-sampler system connected to a 6490 triple quadrupole MS equipped with an electrospray ionization (ESI) source from Agilent jet stream technology. Chromatographic separation was achieved by an analytical Sepax BR-C18 (5 μm, 120 Å 1.0×100 mm) column. The column temperature was maintained at 30°C. The temperature of the auto-sampler was set at 4°C. The sample solutions were injected (2 μL), and the analytes were eluted at a constant flow of 0.150 mL/min of the mobile phase (ratio of acetonitrile to 0.1% formic acid in water, 60:40%, v/v). The isocratic separation run time was 5 min. The MS/MS system was run under negative and/or positive ESI and multiple reactions monitoring (MRM) mode was used to identify the compounds of interest. The operational parameters of MS were: argon as a collision gas; capillary voltage at 5 kV; gas temperature at 225°C; gas flow of 15.1 L/min; and collision energies of 18 and 14 eV for resveratrol and curcumin, respectively. Analyte detection was performed in MRM mode to monitor the precursor to product ion transitions of 226.8-184.8 m/z for resveratrol and 367.1-148.9 for curcumin.

Statistical analysis

Data were expressed as mean ± SD from at least three independent experiments. Statistical comparisons were performed using one-way analysis of variance (ANOVA) with Tukey's multiple comparisons test. The level of statistical significance was set at $*p<0.05$, $**p<0.01$, and $***p<0.001$.

RESULTS

Callus induction and resveratrol content analysis

To induce callus formation, RR was culturedin the 2N6 medium. After three weeks, calli of RR were induced in petri dishes (Fig. 1A). The concentrations of the targeted compounds in the cRR, resveratrol and resveratrol glucoside (piceid), were analyzed using high performance liquid chromatography (HPLC). The retention time of each compound is presented in Fig. 1B-F. The linearity of each compound was calculated using five concentrations of each specific compound. The contents of resveratrol and piceid in cRR were 1.8069 ± 0.0021 μg/g and 66.7641 ± 0.1024 μg/g, respectively (Table 1).

Characterization of micro-cRR and nano-cRR

Micro-cRR and nano-cRR were characterized in terms of size distribution, polydispersity index (PDI), and zeta potential (Table 2). The average hydrodynamic diameter of micro-cRR was greater than 1 μm with a PDI of higher than 0.8. On the other hand, the mean particle size of nano-cRR was approximately 500 nm with a narrow size distribution (PDI<0.5). The zeta potentials of both micro-cRR and nano-cRR were around -14 mV. Together, micro-cRR and nano-cRR exhibit similar physicochemical properties and differ only in size distribution.

In vitro release studies

The *in vitro* release profiles of resveratrol from micro-cRR and nano-cRR were measured at three different conditions, i.e., pH 1.2, 4.5, and 7.4. The cumulative percentage release of resveratrol at each pH condition is shown in Fig. 2, which

Table 1. Piceid and resveratrol contents in NR, RR, cNR and cRR by HPLC

	r^2	Piceid (μg/g)	Resveratrol (μg/g)
NR	0.9991	-	-
RR	0.9995	2.1855 ± 0.0081	0.5404 ± 0.0004
cNR	0.9991	-	-
cRR	0.9991	66.7641 ± 0.1024	1.8069 ± 0.0021

*Values were the means of three replicates ± standard deviation (SD).

Table 2. Size distribution, polydispersity index (PDI), and zeta potential of micro-cRR and nano-cRR

	Size (nm)	PDI	Zeta potential (mV)
Micro-cRR	1625.3 ± 172.5	0.82 ± 0.05	-13.62 ± 0.556
Nano-cRR	485.83 ± 6.717	0.31 ± 0.01	-14.7 ± 0.461

*Values were the means of three replicates ± standard deviation (SD).

illustrates highly pH- and size-dependent release profiles. The release rates of resveratrol from both micro-cRR and nano-cRR were in the order of pH 7.4>4.5>1.2 over 24 h. At pH 7.4, the release rates of resveratrol from micro-cRR and nano-cRR were similar over the time period with about 70% resveratrol released from both formulations. At pH 4.5, the release rate of resveratrol from nano-cRR was significantly higher than that from micro-cRR with approximately 50% and 20% released from nano-cRR and micro-cRR, respectively. At pH 1.2, the release rate of resveratrol from nano-cRR was also significantly higher than that from micro-cRR with approximately 30% and 13% released from nano-cRR and micro-cRR, respectively (Table 3).

The inhibitory effects of micro-cRR and nano-cRR on UVB-induced hyperpigmentation in the skin of brown guinea pigs

To assess whether micro-cRR and nano-cRR have a depigmentation effect, samples were applied topically to the dorsal skin of UVB-irradiated guinea pigs for 15 days. Skin tanning was induced by exposure to UVB irradiation for two weeks. The color index of the UVB (+) group increased by 59.09 compare with that of the UVB (-) group by 52.55. Stimulated melanocytes continuously produced melanin in the epidermis and as a result, the color index of the UVB (+) group reached 72.15 on day 19. After pigmentation was induced by UVB, 200 μL of 1% (w/v) micro-cRR and nano-cRR were treated for 15 days. In addition, nano-callus of normal rice (cNR) was used as a control. Micro-cRR and nano-cRR similarly inhibited melanin production for 12 days. However, the color index of the nano-cRR group has decreased dramatically by 55.1 by day 15 (Fig. 3B).

Inhibitory effect of nano-cRR on the production of melanin granules with Fontana-Masson stain

To visualize melanin, Fontana-Masson staining was carried out on sectioned skin. As shown in Fig. 4A, the amount of melanin granules in the skin of the UVB (+) group increased significantly by 260% compared with those of the UVB (-) group. However, melanin granules produced by UVB overirradiation decreased by 160% from nano-cRR treatment (Fig. 4B).

Resveratrol content in UVB-irradiated dermal skin tissue after treatment with micro-cRR and nano-cRR

Immediately after guinea pigs were sacrificed, skin samples treated with micro-cRR and nano-cRR were collected and fro-

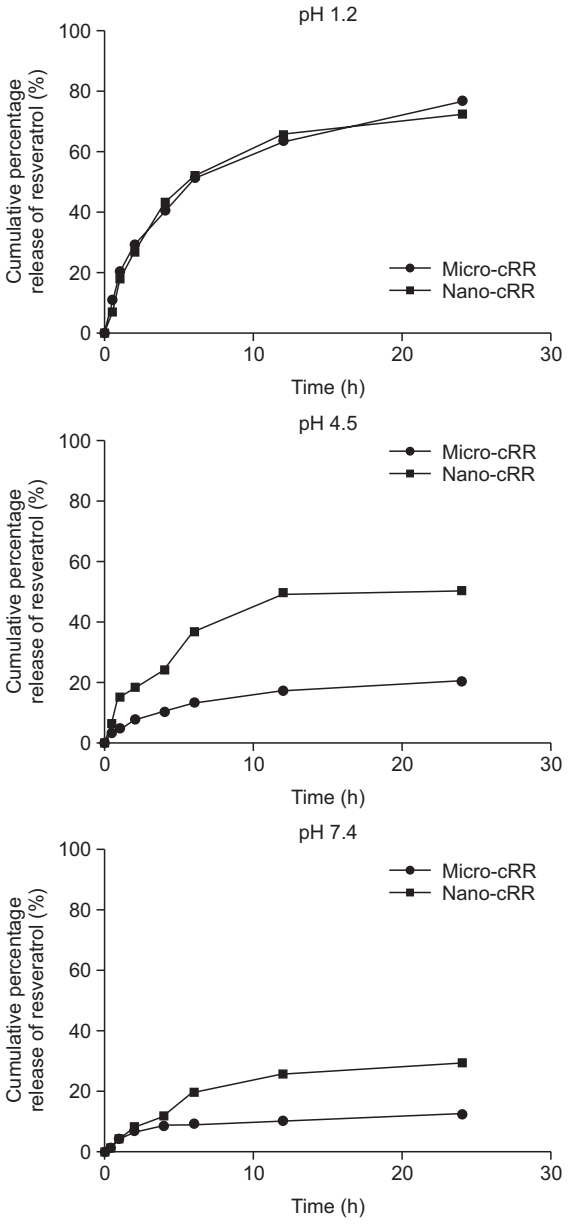

Fig. 2. Cumulative release profiles of resveratrol from micro-cRR and nano-cRR in buffers with different pH.

Table 3. Cumulative percentage release of resveratrol from micro-cRR and nano-cRR at pH 1.2, 4.5, and 7.4

Time (h)	pH 1.2		pH 4.5		pH 7.4	
	Micro-cRR (%)	Nano-cRR (%)	Micro-cRR (%)	Nano-cRR (%)	Micro-cRR (%)	Nano-cRR (%)
0	0	0	0	0	0	0
0.5	11.38	7.03	3.47	6.81	1.57	1.69
1	21.16	18.32	4.99	14.99	4.88	4.82
2	29.64	27.25	7.84	18.51	7.15	8.18
4	40.76	43.55	10.12	24.29	8.73	12.15
6	51.67	52.38	13.19	36.99	9.62	19.99
12	63.78	65.92	17.37	49.33	10.72	26.09
24	76.72	72.65	20.28	50.09	12.84	29.68

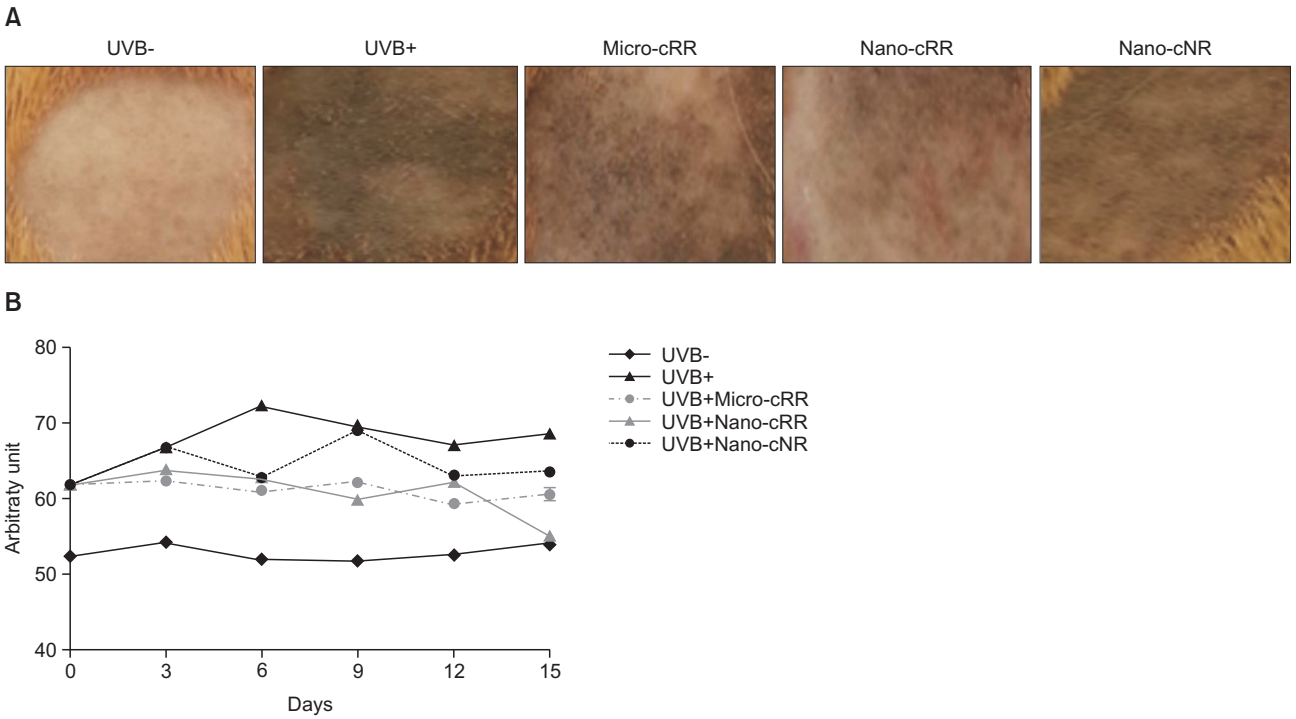

Fig. 3. Effects of nano-cRR on UVB-induced skin pigmentation in brown guinea pigs. (A) Visible decrease in hyperpigmentation. The treated region was divided into 5 areas: UVB-, UVB+, Micro-cRR (1% micro-cRR with UVB), Nano-cRR (1% nano-cRR with UVB), and Nano-cNR (1% nano-cNR with UVB). Representative features of the dorsal skin of brown guinea pigs were obtained after treatment for 15 days. (B) Skin color was measured by a Dermalab® Combo system.

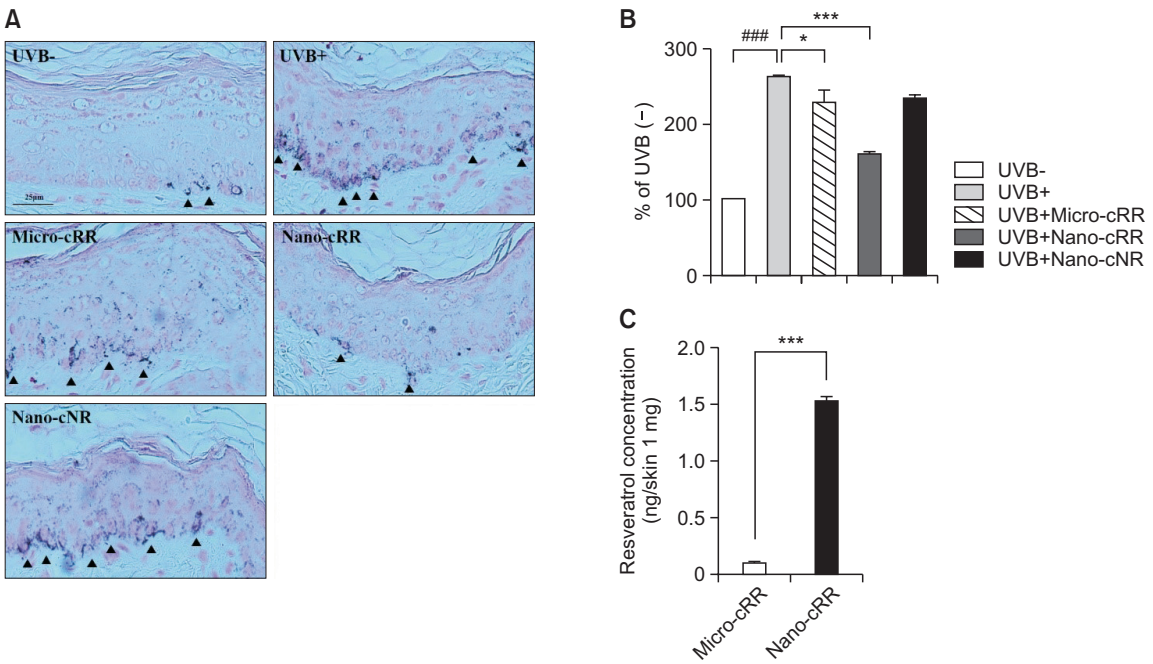

Fig. 4. Histological changes and measurement of filtrated resveratrol in the dorsal skin. (A) Histological examination of the dorsal skin of brown guinea pigs was conducted by Fontana-Masson staining (×200). The arrow heads indicate melanin (B). Densitometry analysis of melanin production was conducted using version 4.0 of the NIS-Elements imaging software. (C) Quantification of filtrated resveratrol in the dorsal skin was measured by LC/MS. The results are the averages of three independent experiments. One-way analysis of variance (ANOVA) with Tukey' multiple comparisons test was used for statistical analyses. $^{###}p<0.001$, $^{*}p<0.05$ and $^{***}p<0.001$ indicate statistically significant differences.

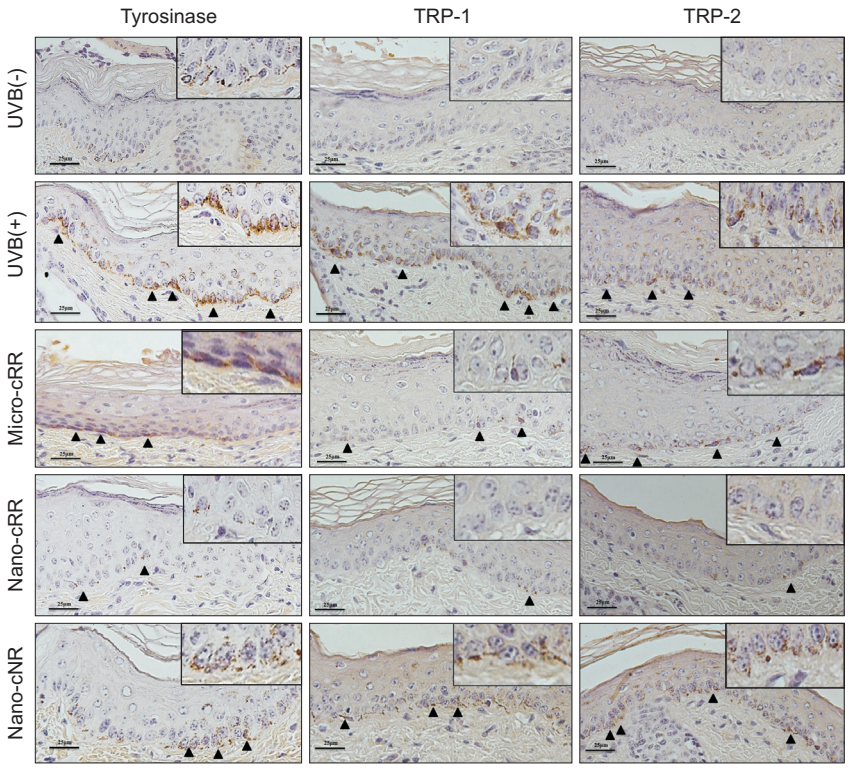

Fig. 5. Expression of tyrosinase, TRP-1, and TRP-2 in paraffin-embedded specimens of UVB-induced skin pigmentation in brown guinea pigs. The expression of tyrosinase, TRP-1, and TRP-2 was evaluated by immunohistochemistry. The arrow heads indicate the expressed proteins.

zen in liquid nitrogen. One hundred milligrams of skin was homogenized and extracted by 100% methanol. The extracted solution was assessed for resveratrol content using LC/MS, revealing that 0.101 ± 0.003 ng and 1.519 ± 0.049 ng of resveratrol were measured in skin treated with micro-cRR and nano-cRR, respectively. We found that skin treated with nano-cRR had a 15-fold higher resveratrol content than that treated with micro-cRR (Fig. 4C).

The inhibitory effects of nano-cRR on the expression of melanogenic proteins in UVB-irradiated brown guinea pig skin

Tyrosinase, tyrosinase-related protein (TRP)-1, and TRP-2 are major proteins that regulate the synthesis of melanin. We analyzed the expression of these proteins by immunohistochemistry of the skin tissues. After UVB irradiation, tyrosinase was highly expressed in the basal layer of the epidermis. Although TRP-1 and TRP-2 were not highly expressed like tyrosinase, they were also increased by UVB stimulation. However, the increase in these melanogenic proteins was significantly inhibited by nano-cRR treatment (Fig. 5).

DISCUSSION

Melanin is a phenolic biopolymer found in the skin, hair, retina, adrenal glands, inner ear, and substantia nigra (Alaluf *et al*., 2002). In humans, melanin has two important functions: to determine the coloration of the skin and hair depending on the amount and type of melanin, and to protect the body against the harmful effects of UV radiation (Slominski *et al*., 2012). However, excessive progress of melanin synthesis is often the cause of hyper-pigmentary disorders (Oh *et al*., 2014). For several years, natural sources that regulate hyperpigmentation have been used in commercial products (Zhong *et al*., 2006; Luo *et al*., 2009; Chang *et al*., 2010; Goh *et al*., 2013).

In this study, we focused on bioresources of nano-calli from resveratrol-enriched rice (RR) with skin whitening activity. Resveratrol is well known as a depigmentation agent that shows anti-melanogenic activities via inhibition of tyrosinase, TRP-1 and TRP-2 expression (Franco *et al*., 2012; Satooka and Kubo 2012; Lee *et al*., 2014a; Park *et al*., 2014). In addition, RR has previously been reported to regulate depigmentation (Lee *et al*., 2014b). We tried to improve the efficacy and biocompatibility of RR using HPH methods by inducing the production of RR calli. We verified the effectiveness of this novel material in UVB-overirradiated dorsal skin of guinea pigs. Recently, several groups have tried to verify the enhancement of active compounds and the bioactive efficacy of calli (Chapagain *et al*., 2008; Cui *et al*., 2010). It is important for plant cell cultures and biomass production to meet the pharmaceutical demands for the development of plant-derived drug resources (Kumar *et al*., 2014). In this study, the content of piceid, a stilbenoid glucoside and a major resveratrol derivative, was increased in the cRR by plant cell cultures. Interestingly, it was recently reported that piceid inhibited melanogenesis in melan-a melanocytes (Jeong *et al*., 2010). We also confirmed inhibitory effect of resveratrol and piceid on the melanin production in

melan-a cells (Supplement 1). Therefore, we expected that calli derived from RR would have potential effects on anti-melanogenesis.

Melanin is synthesized in specialized cells called melanocytes and is relocated to be near keratinocytes by melanosomes (Delevoye 2014). In intracellular organelles known as melanosomes, melanin is made by several enzymes including tyrosinase, TRP-1, and TRP-2, which are involved in the pigmentation pathway (Ramsden and Riley 2014). Currently, the suppression of these enzymes is the main strategy of depigmentation. Particularly, melanocytes are located in the basal layer of the skin epidermis. Therefore, it is very important for active compounds secreted from natural sources to penetrate the skin basal layer. We checked whether resveratrol secreted from cRR could penetrate the skin melanocytes, and whether it interacts with molecular target enzymes such as tyrosinase, TRP-1, and TRP-2. We analyzed the expression of these enzymes in the basal layer of the epidermis by immunohistochemistry. Highly expressed tyrosinase was found in the dermal-epidermal junctions of the skin in the UVB (+) group. In particular, localization of tyrosinase was observed in the perinuclear region of melanocytes. The expression of TRP-1 and TRP-2 shown similar patterns compared to that of tyrosinase. However, nano-cRR treatment remarkably reversed the expression of the melanogenic enzymes. It can be supposed that resveratrol from nano-cRR directly targeted proteins in melanocytes through an increase in the penetrating ratio of the dermal-epidermal junction. Thus, resveratrol secreted from nano-cRR has downregulated the protein level of tyrosinase, TRP-1 and TRP-2. In this study, we found that the secretion of active compounds from nanoparticles of cRR using the HPH technique was increased. Because resveratrol is a polar active compound with depigmentation effect, we assumed that depigmenting efficacy would be depended upon the amount of resveratrol released from raw material. We found that resveratrol released from nano-cRR was more than micro-cRR in PH 4.5. So, we can suggest that nano-cRR may have more potential effect than micro-cRR in normal skin PH range (pH 4.0 to 7.0). The degree of resveratrol released from cRR depends on the molecular size of cRR. Smaller cRR particles are released more quickly and show good anti-melanogenic effects in UVB-induced dorsal skin. It is possible that nano-emulsions of cRR may penetrate the skin better and possess more positive effects than micro-emulsions for anti-melanogenic skin therapy. In fact, nano-cRR showed a greater depigmentation effect than micro-cRR, both visually and histologically. Visually, hyperpigmented skin induced by UVB irradiation was improved to a light brownish color after 15 days of nano-cRR treatment (Fig. 3A). In the histological analysis of Fontana-Masson staining, we observed that melanin production significantly decreased with nano-cRR treatment. In order to support these results, we additionally analyzed the contents of residual resveratrol in the treated skin using an LC/MS system. Higher concentrations of resveratrol were observed in the epidermis and dermis of the nano-cRR group (about 15 times) than in those of the micro-cRR (Fig. 4C).

Taken together, our results demonstrated that nano-cRR suppressed UVB-induced hyperpigmentation by inhibiting tyrosinase, TRP-1, and TRP-2 expression. Our study can therefore conclude that nano-cRR is a promising natural bioresource to act as a whitening agent. Our new approach, namely the induction of calli and the application of high-pressure homogenization (HPH), can be a great alternative for cosmetics, an industry that constantly demands new technologies to be introduced.

ACKNOWLEDGMENTS

This work was supported by a grant from the Next-Generation BioGreen 21 Program (No.PJ01118803), Rural Development Administration, Republic of Korea.

REFERENCES

Alaluf, S., Atkins, D., Barrett, K., Blount, M., Carterv N. and Heath, A. (2002) The impact of epidermal melanin on objective measurements of human skin colour. *Pigment Cell Res.* **15**, 119-126.

Baek, S. H., Chung, H. J., Lee, H. K., D'Souza, R., Jeon, Y., Kim, H. J., Kwon, S. H. and Hong, S. T. (2014) Treatment of obesity with the resveratrol-enriched rice DJ-526. *Sci. Rep.* **4**, 3879.

Baek, S. H., Shin, W. C., Ryu, H. S., Lee, D. W., Moon, E., Seo, C. S., et al. (2013) Creation of resveratrol-enriched rice for the treatment of metabolic syndrome and related diseases. *PloS One.* **8**, e57930.

Chang, M. S., Choi, M. J., Park, S. Y. and Park, S. K. (2010) Inhibitory effects of Hoelen extract on melanogenesis in B16/F1 melanoma cells. *Phytother. Res.* **24**, 1359-1364.

Chapagain, B. P., Saharan, V. and Wiesman, Z. (2008) Larvicidal activity of saponins from Balanites aegyptiaca callus against Aedes aegypti mosquito. *Bioresour. Technol.* **99**, 1165-1168.

Cui, X. H., Chakrabarty, D., Lee, E. J. and Paek, K. Y. (2010) Production of adventitious roots and secondary metabolites by *Hypericum perforatum L*. in a bioreactor. *Bioresour. Technol.* **101**, 4708-4716.

Delevoye, C. (2014) Melanin transfer: the keratinocytes are more than gluttons. *J. Invest. Dermatol.* **134**, 877-879.

Deshpande, A., Dhadi, S. R., Hager, E. J. and Ramakrishna, W. (2012) Anticancer activity of rice callus suspension culture. *Phytother. Res.* **26**, 1075-1081.

Franco, D. C., de Carvalho, G. S., Rocha, P. R., da Silva Teixeira, R., da Silva, A. D. and Raposo, N. R. (2012) Inhibitory effects of resveratrol analogs on mushroom tyrosinase activity. *Molecules* **17**, 11816-11825.

Goh, M. J., Lee, H. K., Cheng, L., Kong, D. Y., Yeon, J. H., et al. (2013) Depigmentation effect of kadsuralignan f on melan-a murine melanocytes and human skin equivalents. *Int. J. Mol. Sci.* **14**, 1655-1666.

Jafarain, A., Asghari, G. and Ghassami, E. (2014) Evaluation of cytotoxicity of *Moringa oleifera* Lam. callus and leaf extracts on Hela cells. *Ad. Biomed. Res.* **3**, 194.

Jeong, E. T., Jin, M. H., Kim, M. S., Chang, Y. H. and Park, S. G. (2010) Inhibition of melanogenesis by piceid isolated from Polygonum cuspidatum. *Arch. Pharm. Res.* **33**, 1331-1338.

Karadag, A., Ozcelik, B. and Huang, Q. (2014) Quercetin nanosuspensions produced by high-pressure homogenization. *J. Agric. Food Chem.* **62**, 1852-1859.

Kumar, M. S., Chaudhury, S. and Balachandran, S. (2014) In vitro callus culture of Heliotropium indicum Linn. for assessment of total phenolic and flavonoid content and antioxidant activity. *Appl. Biochem. Biotechnol.* **174**, 2897-2909.

Lee, T. H., Seo, J. O., Baek, S. H. and Kim, S. Y. (2014a) Inhibitory effects of resveratrol on melanin synthesis in ultraviolet B-induced pigmentation in Guinea pig skin. *Biomol. Ther.* **22**, 35-40.

Lee, T. H., Seo, J. O., Do, M. H., Ji, E., Baek, S. H. and Kim, S. Y. (2014b) Resveratrol-enriched rice down-regulates melanin synthesis in UVB-Induced guinea pigs epidermal skin tissue. *Biomol. Ther.* **22**, 431-437.

Luo, L. H., Kim, H. J., Nguyen, D. H., Lee, H. B., Lee, N. H. and Kim, E. K. (2009) Depigmentation of melanocytes by (2Z,8Z)-matricaria acid methyl ester isolated from *Erigeron breviscapus*. *Biol. Pharm. Bull.* **32**, 1091-1094.

Merisko-Liversidge, E. and Liversidge, G. G. (2011) Nanosizing for

oral and parenteral drug delivery: a perspective on formulating poorly-water soluble compounds using wet media milling technology. *Adv. Drug Deliv. Rev.* **63**, 427-440.

Oh, C. T., Lee, D., Koo, K., Lee, J., Yoon, H. S., Cho, Y. M. et al. (2014) Superoxide dismutase 1 inhibits alpha-melanocyte stimulating hormone and ultraviolet B-induced melanogenesis in murine skin. *Ann. Dermatol.* **26**, 681-687.

Palmero, P., Colle, I., Lemmens, L., Panozzo, A., Nguyen, T. T, Hendrickx, M. and Van Loey, A. (2015) Enzymatic cell wall degradation of high-pressure-homogenized tomato puree and its effect on lycopene bioaccessibility. *J. Sci. Food Agric.* doi:10.1002/jsfa.7088. [Epub ahead of print]

Pandey, H., Pandey, P., Singh, S., Gupta, R. and Banerjee, S. (2015) Production of anti-cancer triterpene (betulinic acid) from callus cultures of different *Ocimum* species and its elicitation. *Protoplasma* **252**, 647-655.

Park, J., Park, J. H., Suh, H. J., Lee, I. C., Koh, J. and Boo, Y. C. (2014) Effects of resveratrol, oxyresveratrol, and their acetylated derivatives on cellular melanogenesis. *Arch. Dermatol. Res.* **306**, 475-487.

Quan, G. L., Chen, B., Wang, Z. H., Wu, H., Huang, X. T., Wu, L. N. and Wu, C. B. (2012) Improving the dissolution rate of poorly water-soluble resveratrol by the ordered mesoporous silica. *Yao Xue Xue Bao* **47**, 239-243.

Ramsden, C. A. and Riley, P. A. (2014) Tyrosinase: the four oxidation states of the active site and their relevance to enzymatic activation, oxidation and inactivation. *Bioorg. Med. Chem.* **22**, 2388-2395.

Satooka, H. and Kubo, I. (2012) Resveratrol as a kcat type inhibitor for tyrosinase: potentiated melanogenesis inhibitor. *Bioorg. Med. Chem.* **20**, 1090-1099.

Shelar, D., Pawar, S. and Vavia, P. (2013) Fabrication of isradipine nanosuspension by anti-solvent microprecipitation-high-pressure homogenization method for enhancing dissolution rate and oral bioavailability. *Drug Deliv. Transl. Res*. **3**, 384-391.

Siddique, A. B., Ara, I., Islam, S. M. and Tuteja, N. (2014) Effect of air desiccation and salt stress factors on in vitro regeneration of rice (*Oryza sativa* L.). *Plant Signal. Behav.* **9**, e977209.

Slominski, A. T., Zmijewski, M. A, Skobowiat, C., Zbytek, B., Slominski, R. M. and Steketee, J. D. (2012) Sensing the environment: regulation of local and global homeostasis by the skin's neuroendocrine system. *Adv. Anat. Embryol. Cell Biol.* **212**, v, vii, 1-115.

Zhong, S., Wu, Y., Soo-Mi, A. Zhao, J., Wang, J., Yang, S., et al. (2006) Depigmentation of melanocytes by the treatment of extracts from traditional Chinese herbs: a cell culture assay. *Biol. Pharm. Bull*. **29**, 1947-1951.